*Journal of Experimental Botany*, Vol. 60, No. 1, pp. 197–212, 2009
doi:10.1093/jxb/ern280 Advance Access publication 27 November, 2008
This paper is available online free of all access charges (see http://jxb.oxfordjournals.org/open_access.html for further details)

Journal of Experimental Botany
www.jxb.oxfordjournals.org

RESEARCH PAPER

# An isoform of myosin XI is responsible for the translocation of endoplasmic reticulum in tobacco cultured BY-2 cells

**Etsuo Yokota[1,*], Shunpei Ueda[1], Kentaro Tamura[2], Hidefumi Orii[1], Satoko Uchi[1], Seiji Sonobe[1], Ikuko Hara-Nishimura[2] and Teruo Shimmen[1]**

[1] Department of Life Science, Graduate School of Life Science, University of Hyogo, Harima Science Park City, Hyogo 678-1297, Japan
[2] Department of Botany, Graduate School of Science, Kyoto University, Sakyo-ku, Kyoto 606-8502, Japan

Received 18 July 2008; Revised 14 October 2008; Accepted 16 October 2008

## Abstract

**The involvement of myosin XI in generating the motive force for cytoplasmic streaming in plant cells is becoming evident. For a comprehensive understanding of the physiological roles of myosin XI isoforms, it is necessary to elucidate the properties and functions of each isoform individually. In tobacco cultured BY-2 cells, two types of myosins, one composed of 175 kDa heavy chain (175 kDa myosin) and the other of 170 kDa heavy chain (170 kDa myosin), have been identified biochemically and immunocytochemically. From sequence analyses of cDNA clones encoding heavy chains of 175 kDa and 170 kDa myosin, both myosins have been classified as myosin XI. Immunocytochemical studies using a polyclonal antibody against purified 175 kDa myosin heavy chain showed that the 175 kDa myosin is distributed throughout the cytoplasm as fine dots in interphase BY-2 cells. During mitosis, some parts of 175 kDa myosin were found to accumulate in the pre-prophase band (PPB), spindle, the equatorial plane of a phragmoplast and on the circumference of daughter nuclei. In transgenic BY-2 cells, in which an endoplasmic reticulum (ER)-specific retention signal, HDEL, tagged with green fluorescent protein (GFP) was stably expressed, ER showed a similar behaviour to that of 175 kDa myosin. Furthermore, this myosin was co-fractionated with GFP–ER by sucrose density gradient centrifugation. From these findings, it was suggested that the 175 kDa myosin is a molecular motor responsible for translocating ER in BY-2 cells.**

**Key words:** Actin, endoplasmic reticulum, myosin XI, tobacco cultured cell.

## Introduction

Myosins, actin-based molecular motors in eukaryotic cells, are involved in various cellular functions such as muscle contraction, cytokinesis, cell and organelle movement, membrane trafficking, and signal transduction (Mermall *et al.*, 1998). They are divided into at least 24 classes on the basis of the primary structure of the heavy chain gene (Foth *et al.*, 2006). In general, a heavy chain has three regions, an N-terminal head region containing a motor domain, a neck region with a light chain-binding domain such as an IQ motif, and a C-terminal tail region in which primary structures and sizes are diverse within each class of myosin (Korn, 2000).

From plant cells, three classes of myosin, VIII, XI, and XIII, have been identified from the molecular biological view point thus far (Reichelt and Kendrick-Jones, 2000; Reddy, 2001). Myosin VIII, which was identified first from *Arabidopsis thaliana* (Knight and Kendrick-Jones, 1993), has been shown to be localized at the surface of the plasma membrane, especially at newly synthesized cell walls and plasmodesmata in higher plant cells (Baluska *et al.*, 2001; Volkmann *et al.*, 2003). Although the motile and ATPase activities of myosin VIII have not yet been characterized, it is hypothesized that this myosin is involved in regulation of the pore size of plasmodesmata. Recently, this myosin class was found to be co-localized on endocytotic vesicles, and was assumed to be involved in their translocation (Golomb *et al.*, 2008). In the case of myosin XIII identified from the green alga *Acetabularia*, no biochemical property has yet

* To whom correspondence should be addressed. E-mail: yokota@sci.u-hyogo.ac.jp

been demonstrated. However, based on an immunolocalization study showing the association of this myosin with organelles and vesicles in *Acetabularia* cells, it was suggested that myosin XIII is a molecular motor for cytoplasmic streaming (Vugrek *et al.*, 2003).

Myosin XI has been identified from *Arabidopsis* and was grouped with myosin V when first discovered (Kinkema and Shiefelbein, 1994; Kinkema *et al.*, 1994). In *Arabidopsis*, myosin XI was shown to form a large gene family with a total of 13 isoforms (Reddy and Day, 2001). Unlike myosin VIII and XIII, the biochemical and biophysical properties of some isoforms of class XI myosin have been well characterized by studies using native protein fractions isolated from plant cells such as lily pollen, tobacco cultured BY-2 cells, and *Chara* internodal cells (Shimmen and Yokota, 2004). The native myosin XI is able to translocate F-actin by motile analysis *in vitro* with a velocity consistent with that of cytoplasmic streaming observed in living plant cells. Pharmacological studies using actin-depolymerizing drugs, cytochalasins or latrunculins, or an inhibitor of myosin activity, 2,3-butanedione monoxime (BDM), demonstrated that the actin–myosin system contributes to the translocation or movement of the peroxisome (Collings *et al.*, 2002, 2003; Jedd and Chua, 2002; Mano *et al.*, 2002; Mathur *et al.*, 2002), Golgi (Boevink *et al.*, 1998; Nebenfuhr *et al.*, 1999), mitochondrion (Logan and Leaver, 2000; Van Gestel *et al.*, 2002), chloroplast (Wada *et al.*, 2003; Paves and Truve, 2007), plastid (Kwok and Hanson, 2003), vacuole (Higaki *et al.*, 2006), and endoplasmic reticulum (ER; Knebel *et al.*, 1990; Quader, 1990; Liebe and Menzel, 1995; Boevink *et al.*, 1998) in higher plant cells. Immunocytochemical studies using an antibody against myosin XI heavy chain revealed that myosin XI is localized on mitochondria and plastids in root cells of maize (Liu *et al.*, 2001; Wang and Pesacreta, 2004), mitochondria and vesicles in tobacco pollen tubes (Romagnoli *et al.*, 2007), and peroxisomes in *Arabidopsis* (Hashimoto *et al.*, 2005). When a fluorescence protein-tagged tail region of several myosin XI isoforms was expressed in tobacco, onion (Reisen and Hanson, 2006), and *Arabidopsis* cells (Li and Nebenfuhr, 2007), Golgi and peroxisomes were decorated. In some cases, the movement of these organelles and mitochondria was reported to be suppressed or modified by the expression of the tail region (Avisar *et al.*, 2008; Peremyslov *et al.*, 2008). Furthermore, the transport and movement of Golgi, mitochondria, and peroxisomes were suppressed or modified by the knockout of certain isoforms of myosin XI in tobacco (Avisar *et al.*, 2008) and *Arabidopsis* cells (Peremyslov *et al.*, 2008). These studies indicate the involvement of myosin XI in the movement of various types of organelles in plant cells.

It has been revealed that two kinds of myosins, composed of a 175 kDa (175 kDa myosin) and 170 kDa heavy chain (170 kDa myosin), a homologue of lily 170 kDa myosin (Yokota and Shimmen, 1994), are present in tobacco cultured BY-2 cells (Yokota *et al.*, 1999) and belong to myosin class XI (Yokota *et al.*, 2001; Tominaga *et al.*, 2003). Total amino acid sequence comparison of the 175 kDa myosin heavy chain (accession no. AB082121) with that of the 170 kDa myosin heavy chain (accession no. AB180675) showed 63% identity. The 175 kDa myosin heavy chain exhibited relatively higher identity of 75% with MYA2 (accession no. Z34293) than with another isoform of *Arabidopsis* myosin XI, MYA1 (60%; accession no. Z28389). On the other hand, the 170 kDa myosin heavy chain had higher identity with MYA1 (74%) than MYA2 (61%). Native 175 kDa myosin isolated biochemically was able to translocate F-actin in the motility assay *in vitro* with a velocity of ~6–9 μm $s^{-1}$ (Yokota *et al.*, 1999; Tominaga *et al.*, 2003). This velocity was consistent with the highest velocity of cytoplasmic streaming observed in intact BY-2 cells. On the other hand, the sliding velocity of F-actin *in vitro* induced by a fraction containing 170 kDa myosin (2–4 μm $s^{-1}$) was comparable with the low velocity of cytoplasmic streaming in BY-2 cells. These results imply that both myosins are involved in cytoplasmic streaming in BY-2 cells.

The 175 kDa myosin heavy chain had six IQ motifs (Tominaga *et al.*, 2003), putative calmodulin- (CaM) binding regions, which are considered to confer $Ca^{2+}$ sensitivity to this myosin activity. Indeed, 175 kDa myosin was associated with CaM, and its motile activity *in vitro* was suppressed by the micromolar concentrations of $Ca^{2+}$ (Yokota *et al.*, 1999; Tominaga *et al.*, 2004). This myosin had two heads and a tail with two small globular structures, indicating the dimerization of two heavy chains through α-helical coiled-coil domains residing in the N-terminus of the tail region (Tominaga *et al.*, 2003). The optical trap nanometry assay revealed that a single 175 kDa myosin molecule moves processively along an actin filament in 35 nm steps with high velocity (Tominaga *et al.*, 2003). Hence, the 175 kDa myosin is thought to be a suitable and ideal motor for organelle transport in cytoplasmic streaming, since it is expected that this myosin can effectively translocate the cargo along actin filaments for long distances without becoming detached from them due to its processivity, like myosin V (Reck-Peterson *et al.*, 2000) and VI (Frank *et al.*, 2004), which are involved in organelle transport and membrane trafficking in animal and yeast cells. Recently, MYA1 was also suggested to be a processive motor based on enzymatic activities shown by its recombinant head region (Hachikubo *et al.*, 2007). However, it remains to be elucidated which organelles or vesicles are translocated by 175 kDa myosin. The present study demonstrated that the 175 kDa myosin is responsible for the translocation of ER based on immunolocalization analysis using an antibody against myosin heavy chain and BY-2 cells, in which green fluorescent protein (GFP)-labelled ER is stably expressed.

## Materials and methods

### *Culture and synchronization of BY-2 cells*

BY-2 cells were cultured by the method of Nagata *et al.* (1981). The positional correlation between 175 kDa myosin

or 170 kDa myosin and ER was examined using a BY-2 stain transformed with a chimeric gene constructed from the signal peptide of pumpkin 2S albumin, GFP, and the ER retention signal (HDEL), and showed a strong and stable fluorescence on the ER network (Mitsuhashi *et al.*, 2000).

For synchronization, cells from 7-d-old cultures were first synchronized by treatment with aphidicolin for a one-step synchronization procedure and then further with propyzamide for a two-step synchronization procedure according to the method of Kakimoto and Shibaoka (1988). In brief, cells were treated with 4.5 μg $ml^{-1}$ aphidicolin (Wako Pure Chemical Industries) for 24 h with agitation at 160 rpm at 27 °C. After washing three times with 3% sucrose, the cells were cultured in the basal medium for 6 h and then treated with 4.8 μM propyzamide (Wako) for 5 h. After washing three times, the cells were cultured in the basal medium. For the one-step synchronization procedure, the cells were treated with aphidicolin for 24 h. After washing, the cells were cultured in the basal medium for 6–7 h. To examine the effect of BDM, cells were treated with BDM (Sigma) at a final concentration of 50 mM in the basal medium after the aphidicolin or propyzamide treatment.

### *Isolation of phragmoplasts*

Isolation of phragmoplasts from synchronized cells was carried out by the method of Kakimoto and Shibaoka (1988) with some modifications. All steps were done at room temperature. After the propyzamide treatment, the cells were cultured in the basal medium for 60–90 min. $NaN_3$ at a final concentration of 0.1% was added to the cultivate. After 2 h, the cells were collected by centrifugation at 2000 *g* for 2 min and suspended in a solution containing 1% cellulase ONOZUKA RS (Yakult), 0.1% pectolyase Y23 (Seishin Pharmaceutical), and 0.4 M sorbitol (pH 5.5). After 2 h, protoplasts were collected by centrifugation and washed three times with 0.6 M sorbitol. Protoplasts were suspended in EMP solution [10 mM EGTA, 6 mM $MgCl_2$, 1 mM dithiothreitol (DTT), 100 μg $ml^{-1}$ leupeptin, 1 mM phenylmethylsulphonyl fluoride (PMSF), and 50 mM PIPES-KOH (pH 7.0)] supplemented with 0.05% Triton X-100 and 1% casein. After centrifugation at 1000 rpm for 5 min, the pellet was washed twice with the EMP solution. The sample (crude phragmoplast fraction) was suspended in the EMP solution and then mixed with the same volume of 40% Percoll (pH 7.3; GE Healthcare Bio-Sciences AB). After centrifugation at 16 000 *g* for 30 min, fractions containing phragmoplasts were pooled and centrifuged at 28 000 *g* for 10 min. The pellet was washed twice with the EMP solution and then suspended in it. This was used as the isolated phragmoplast fraction.

### *Isolation of ER*

GFP–ER was isolated from BY-2 cells by sucrose density gradient ultracentrifugation according to the method of Dong *et al.* (1988) with some modifications. The following procedures were carried out at 0–4 °C. Protoplasts were homogenized in a homogenization buffer [8 mM EGTA, 1 mM $MgCl_2$, 1% casein, 0.3 M sucrose, 0.5 mM DTT, 1 mM PMSF, 50 μg $ml^{-1}$ leupeptin, and 40 mM PIPES-KOH (pH 7.0)] by six strokes with a hand-operated Downs homogenizer. The homogenate was centrifuged at 500 *g* for 3 min. The supernatant was further centrifuged at 12 000 *g* for 10 min. The supernatant containing the microsomal fraction and cytosol was centrifuged on a 0.6, 1.0, and 1.5 M discontinuous sucrose density gradient made up in a solution containing 5 mM EGTA, 1 mM $MgCl_2$, 0.5 mM DTT, 1 mM PMSF, 50 μg $ml^{-1}$ leupeptin, and 30 mM PIPES-KOH (pH 7.0) at 86 000 *g* for 1.5 h. The interfaces between the 0.6 M and 1.0 M, and the 1.0 M and 1.5 M sucrose were recovered and analysed. In the case of the ultracentrifugation of the continuous sucrose density gradient from 1.6 M (bottom) to 0.5 M (top), fractions were collected from the bottom and divided into 27 fractions. A fraction immobilized in and floating on the sucrose gradient was also collected and is shown as S in Fig. 7B.

### *Preparation of antibodies*

The 175 kDa myosin isolated from BY-2 cells (Yokota *et al.*, 1999) was subjected to SDS–PAGE according to the method of Laemmli (1970). After slight staining of gels with Coomassie brilliant blue (CBB), bands of myosin heavy chain were excised and homogenized in Titer Max Gold (TiterMax, USA). The homogenate was injected into a male rabbit. A total of three boosts were given at 2-week intervals. The animal was bled 2 weeks after the final injection. The serum was stored frozen at –80° C until used. Affinity-purified antibody against 175 kDa heavy chain from the serum was prepared according to a method described previously (Yokota *et al.*, 1995*a*), using the 175 kDa myosin heavy chain transferred on a PVDF-nitrocellulose membrane (polyvinyldifluoride immobilon membrane; Millipore).

### *Immunoblotting*

After SDS–PAGE, proteins in the gel were electrophoretically transferred to a PVDF-nitrocellulose sheet according to the method of Towbin *et al.* (1979). Antigens on the nitrocellulose membrane were detected as described previously (Yokota *et al.*, 1995*a*). An antiserum against 175 kDa myosin heavy chain or 170 kDa myosin heavy chain (Yokota and Shimmen, 1994), an antibody against GFP (rabbit polyclonal antibody; Merck Calbiochem), actin (clone C4; ICN), α-tubulin (Ab-1; OncogeneTM Reseach Products), or alkaline phosphatase-conjugated anti-rabbit IgG (Sigma) were diluted 1000-, 1000-, 1000-, 2000-, 1000-, 1000-, or 3000-fold, respectively, with phosphate-buffered saline (PBS) supplemented with 2% (w/v) bovine serum albumin (BSA) and 0.05% (v/v) Tween-20. Affinity-purified antibody against 175 kDa myosin or 170 kDa myosin heavy chain (Yokota *et al.*, 1995*a*) was diluted 50-fold and used for immunoblot analysis. A crude protein sample was prepared from BY-2 cells using

a trichloroacetic acid (TCA) precipitation method according to Yokota and Shimmen (1994).

### *Preparation of samples for immunofluorescence microscopy*

BY-2 cells were immunostained by the method of Yokota *et al.* (1995*a*, *b*) with some modifications. BY-2 cells were treated for 12 min with an enzyme solution containing 1% (w/v) cellulase (R-10; Yakult), 0.5% (w/v) pectinase (Macerozyme R-10; Yakult), and 0.3 M mannitol at room temperature. After washing with 0.3 M mannitol, the cells were allowed to adhere to polylysine-coated glass slides and were fixed with 3.5% (w/v) paraformaldehyde in PME [50 mM PIPES-KOH, 2 mM $MgSO_4$, and 5 mM EGTA (pH 6.9)] for 1 h. After several rinses with PME, the cells were treated with 0.5% (v/v) Triton X-100 in PME for 10 min. After several washes with PBS, the cells were incubated in a mixture of antibodies against 175 kDa or 170 kDa myosin heavy chain and α-tubulin diluted 20- or 200-fold, respectively, with PBS supplemented with 2% (w/v) BSA at room temperature for 1 h. For double staining with antibody against each myosin heavy chain and fluorescent phalloidin [rhodamine–phalloidin (RP) or Bodipy FL phallacidin: Invitrogen], the cells were incubated with each antibody alone. The cells were washed with PBS and treated with secondary antibody, which had been conjugated with Alexa fluor 488 or 594 (Invitrogen), at room temperature for 1 h in the dark. For staining actin filaments, RP or Bodipy FL phallacidin was mixed with secondary antibody. Alexa fluor-conjugated antibodies or fluorescence phalloidin was diluted 100- or 50-fold, respectively, with PBS supplemented with 2% (w/v) BSA. After several washes, the cells were mounted in a medium containing 50% (v/v) glycerol, 1 μg $ml^{-1}$ Hoechst 33258 (Sigma), and 50 mM TRIS-HCl (pH 7.6). Samples were examined with an Axioskop microscope (Carl Zeiss) equipped with epifluorescence optics or a laser scanning microscope (LSM-510; Carl Zeiss). For immunostaining of isolated phragmoplasts and the GFP–ER fraction, these samples were allowed to adhere to polylysine-coated glass slides, fixed, and treated with antibodies in the same manner as described above.

### *Other inhibitors*

Oryzalin (Riedel-de Haen) and latrunculin B (Merck Calbiochem) were dissolved in dimethylsulphoxide (DMSO) at 20 mM and 5 mM, respectively, as stock solutions.

## Results

### *Each myosin XI isoform associates with different organelles in BY-2 cells*

In the present study, we immunized a rabbit against 175 kDa heavy chain isolated biochemically, and affinity-purified an antibody from the serum. This antibody specifically cross-reacted with 175 kDa myosin heavy chain in a crude protein sample prepared from BY-2 cells (Supplementary Fig. S1 available at *JXB* online), like an affinity-purified mouse antibody used in a previous study (AAB-175; Yokota *et al.*, 1999). First, the localization of each isoform of myosin XI, 175 kDa and 170 kDa myosin, was examined in interphase cells. The antibody against 170 kDa myosin used in the present study was the same one used in previous studies (Yokota *et al.*, 1995*a*, *b*, 1999). Bright signals of 175 kDa myosin were observed as fine dots throughout the cytoplasm (Fig. 1A, 1B), while signals of 170 kDa myosin appeared as relatively large dots and were distributed throughout the cytoplasm (Fig. 1C). In the cortical region, fine dots of 175 kDa myosin signals were not dispersed evenly. Thus, each myosin is associated with a different cargo in BY-2 cells. During the observation, it was noticed that signals of 175 kDa myosin were concentrated in an equatorial plane in the mitotic cell, but the frequency of mitotic cells was much lower than that of interphase cells. Hence, the localization of 175 kDa myosin was examined in mitotic cells synchronized by a two-step procedure.

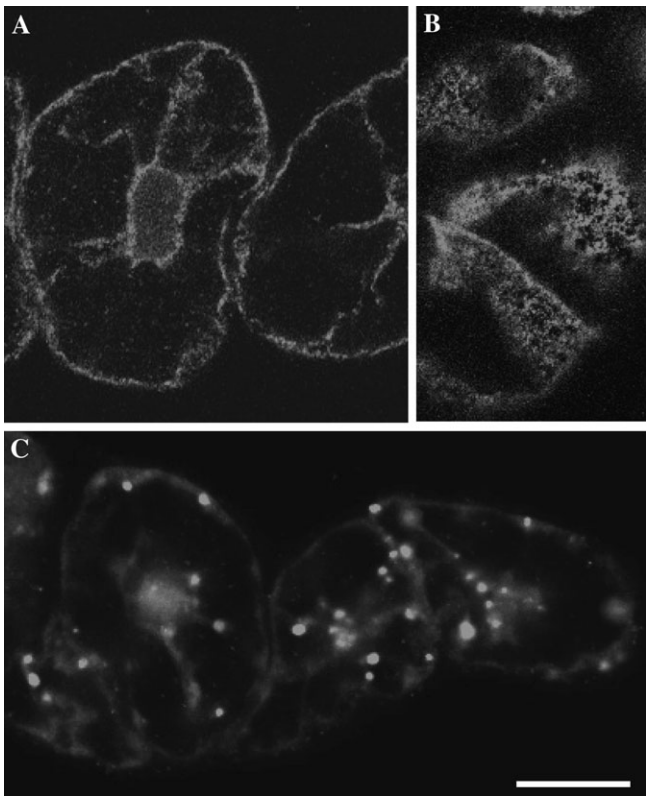


**Fig. 1.** Localization of 170 kDa and 175 kDa myosin in interphase BY-2 cells. Immunofluorescence staining was carried out using the antibody against 175 kDa myosin (A and B) or 170 kDa myosin heavy chain (C). A and C are focused at nuclear regions, while B is focused at the cortical region. The bright signals of 175 kDa myosin were observed as fine dots dispersed throughout the cytoplasm, and appeared to be mesh-like clusters of dots in the cortical region. The signals of 170 kDa myosin were observed on larger organelles. The bar represents 20 μm.

*The 175 kDa myosin accumulates in the phragmoplast during mitosis*

To determine the stage of mitosis, synchronized cells were treated with Hoechst for staining condensing chromatin, together with antibodies against myosin heavy chain and tubulin or RP. First, the distribution of microtubule and 175 kDa myosin during mitosis was analysed (Fig. 2, and and Supplementary Fig. S2 at *JXB* online). In metaphase cells, the 175 kDa myosin (Fig. 2A, and Supplementary S2A, B) was localized throughout the cytoplasm including the spindle region (Fig. 2a, and Supplementary Fig. S2a, b). During the assembly of the phragmoplast, some parts of 175 kDa myosin accumulated in the equatorial plane (triangles in Fig. 2B, C, and Supplementary Fig. S2C–F). Other parts of this myosin were detected around daughter nuclei (arrows in Fig. 2B, C, and Supplementary Fig. S2D–F). In the phragmoplast, the 175 kDa myosin band (triangles in Fig. 2D, and Supplementary Fig. S2F–H) in the equatorial plane overlapped with the boundary between the opposite microtubule bundles (Fig. 2d, and Supplementary Fig. S2f–h). Near the end of mitosis when microtubule bundles (Fig. 2e, and Supplementary Fig. S2i, j) in the phragmoplast started to become disorganized, the 175 kDa myosin in the equatorial plane also started to diffuse (triangles in Fig. 2E, and Supplementary Fig. S2J). They continued to aggregate around daughter nuclei in late telophase (arrows in Fig. 2D, E, and Supplementary Fig. S2G–I).

The correlation between 175 kDa myosin and actin filament distribution during mitosis is shown in Fig. 3 and Supplementary Fig. S3 at *JXB* online. The 175 kDa myosin became dispersed in the spindle region in the metaphase cell, but did not appear in a region where chromosomes were aligned (triangles in Fig. 3A, and Supplementary Fig. S3A, B). Cytoplasmic strands also contained the 175 kDa myosin (arrows in Fig. 3A, and Supplementary Fig. S3A, B). Filamentous and diffuse signals of RP were observed in and around the spindle region (Fig. 3a, and Supplementary Fig. S3a, b). During the progression of mitosis, signals of both 175 kDa myosin (Fig. 3B–D, and Supplementary Fig. S3C–H) and RP (Fig. 3b–d, and Supplementary Fig. S3c–h) were concentrated in the mid plane between segregating daughter chromosomes or daughter nuclei (triangles in Fig. 3B–D, and Supplementary

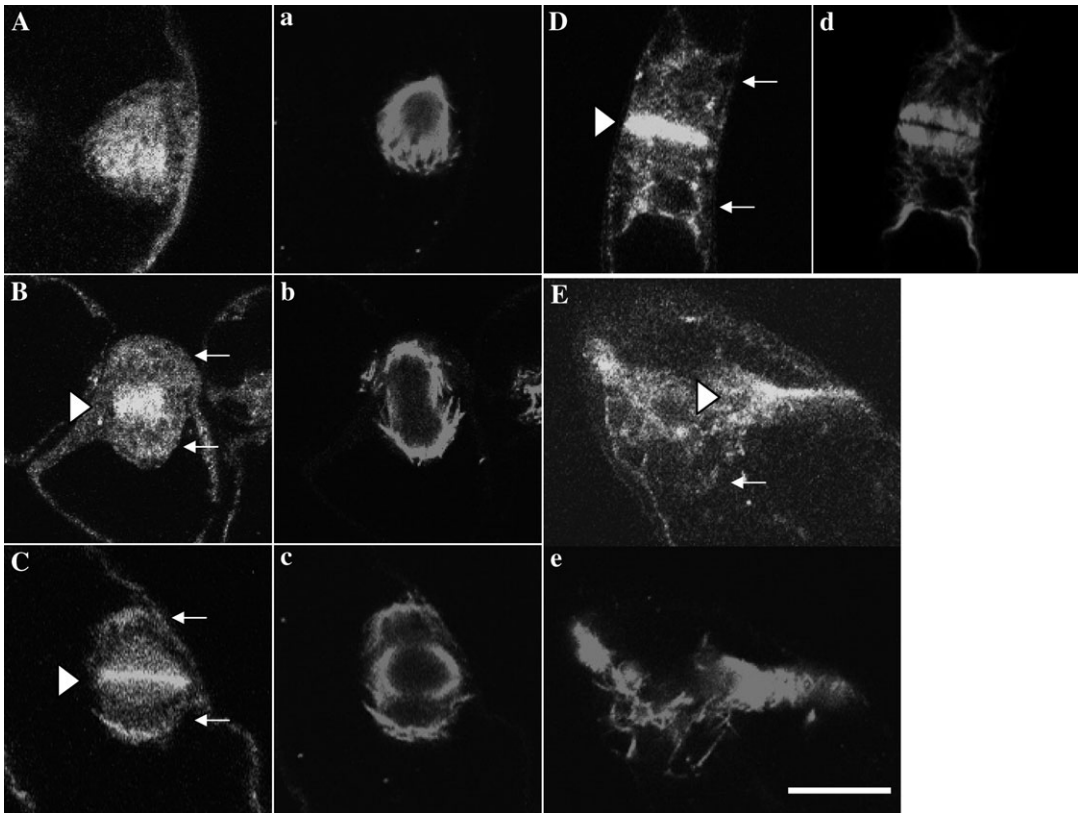


**Fig. 2.** Localization of 175 kDa myosin and microtubules in mitotic BY-2 cells. Double immunofluorescence staining was carried out using antibodies against tubulin (lower case letters) and 175 kDa myosin heavy chain (upper case letters). In metaphase, signals of 175 kDa myosin (A) were found in the spindle region (a). During the segregation of daughter chromosomes and the assembly of phragmoplast (b and c), the 175 kDa myosin accumulated in the mid plane (triangle in B) and equatorial plane (triangle in C), and also located around daughter nuclei (arrows in B and C). In mature phragmoplast (d), the 175 kDa myosin was further concentrated in the equatorial plane and formed the band-like structure (triangle in D). This myosin continued to surround the daughter nuclei (arrows in D and E). When the phragmoplast became disorganized (e), the 175 kDa myosin was released from the equatorial plane (triangle in E). The bar represents 20 μm.

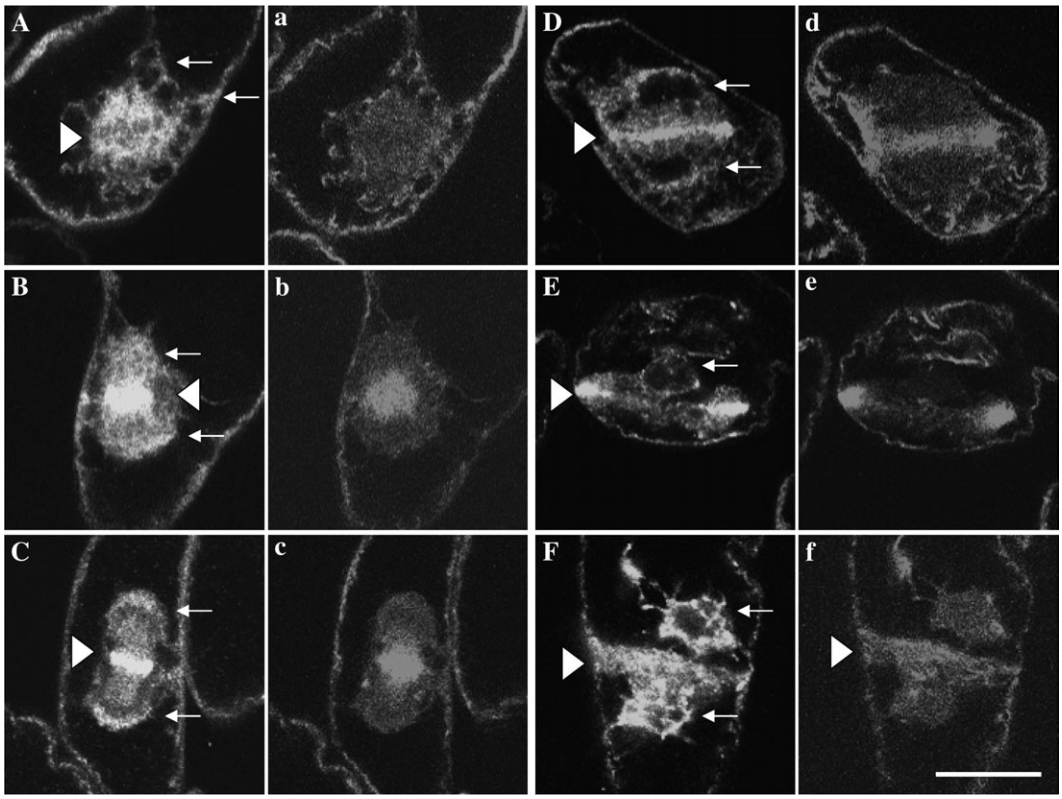


**Fig. 3.** Localization of 175 kDa myosin and actin filament in mitotic cells. Double immunofluorescence staining was carried out using the antibody against 175 kDa myosin (upper case letters) and RP (lower case letters). In metaphase cells, some parts of the 175 kDa myosin were present in the spindle region (A), where diffuse and filamentous signals of RP were found (a). The triangle and arrows indicate the position of aligned chromosomes in the mid plane and cytoplasmic strands, respectively. During the progression of mitosis, 175 kDa myosin accumulated in the equatorial plane (triangles in B and C) and was also observed around daughter nuclei (arrows in B and C). Concomitantly, bright bands of RP signals emerged in the equatorial plane (b and c), which corresponded to actin filament bundles in the phragmoplast. The 175 kDa myosin was further concentrated in the equatorial region in the developed phragmoplast (triangle in D) and also surrounded the daughter nuclei (arrows in D and E), where only diffuse RP signals were observed (d). At this stage, the band of RP signals in the equatorial plane became narrower (d). In the centre of the equatorial plane, only a small amount of 175 kDa myosin (E) and signals of RP (e) were present, whereas bright signals of both components were observed at the margin (triangle in E). In the late telophase cells, both components were dispersed from the equatorial plane (triangles in F and f) and diffused to the cytoplasm. Arrows in F indicate daughter nuclei. The bar represents 20 μm.

Fig. S3C–H), where the phragmoplast was constructed. The band of 175 kDa myosin (triangles in Fig. 3C, D, and Supplementary Fig. S3C–H) in the equatorial plane of the phragmoplast was generally narrower than that of the RP signal (Fig. 3c, d, and Supplementary Fig. S3c–h) and seemed to overlap with the boundary between opposite actin filament bundles, although the boundary was less clear in the chemically fixed cells of the present study. Signals of both elements (Fig. 3E for 175 kDa myosin and Fig. 3e for actin filament) were brighter and more intense at the margin (triangle in Fig. 3E) than those in the centre of the equatorial plane in the phragmoplast. Near the end of or after mitosis, both elements (Fig. 3F for 175 kDa myosin and Fig. 3f for actin filaments) diffused from the equatorial plane (triangles in Fig. 3F, f) and became dispersed in the cytoplasm. Around segregated daughter chromosomes or daughter nuclei (arrows in Fig. 3B–F, and Supplementary S3C–H), the 175 kDa myosin was also distributed as described above.

To analyse further the positional correlation between 175 kDa myosin and actin filament bundles in the phragmoplast, the localization of both elements in isolated phragmoplasts from mitotic cells was examined. Immunoblotting showed the presence of the 175 kDa myosin in isolated phragmoplasts (lane d in Fig. 4A) as well as the main components of the phragmoplast, actin and tubulin (lanes b and c in Fig. 4A, respectively), but not 170 kDa myosin (lane e in Fig. 4A). In the isolated phragmoplast, the 175 kDa myosin (panel a in Fig. 4B, and Supplementary Fig S4A–C at *JXB* online) was concentrated at the boundary between the opposite bundles of actin filaments (panel b in Fig. 4B, and Supplementary Fig. S4a–c; panel c in Fig. 4B is a merged image of panel a and b) or microtubules (Supplementary Fig. S4E–G for the 175 kDa myosin; Supplementary Fig. S4e–g for microtubules), where actin filaments or microtubules appeared to be depleted (arrows in Fig. 4B, and Supplementary Fig. S4). However, since the width of the 175 kDa myosin band was slightly larger than

that of the boundary of actin filament bundles, the edges of the 175 kDa myosin band overlapped with actin filament bundles (panel c in Fig. 4B). In a polar view of the isolated phragmoplast, the 175 kDa myosin (panel d in Fig. 4B) was co-localized with the actin filament ring (panel e in Fig. 4B), and a few of both elements were observed inside the ring, where the cell plate was newly formed.

### *ER and 175 kDa myosin show similar behaviour in interphase and during mitosis*

Ultrastructural (Hepler, 1980, 1982), immunocytochemical (Napier *et al.*, 1992; Denecke *et al.*, 1995), and GFP fluorescence microscopic analyses (Nebenfuhr *et al.*, 2000; Higaki *et al.*, 2008) have revealed that ER gathers in the spindle region in the metaphase and then is accumulated in the phragmoplast and around daughter nuclei during mitosis. To examine a positional correlation between 175 kDa myosin and ER in interphase and mitotic cells, immunostaining with the anti-175 kDa myosin antibody was performed using BY-2 cells, in which GFP-labelled ER (GFP–ER) is expressed (Mitsuhashi *et al.*, 2000).

In interphase cells, GFP–ER was distributed throughout cytoplasmic strands emanating from the nuclear region and penetrating the vacuole (Fig. 5A). The GFP–ER in the cytoplasm in the living cell moved and streamed with an average velocity of ~7 μm $s^{-1}$, ranging from 4 μm $s^{-1}$ to 9 μm $s^{-1}$. In the cortical region, ER was arranged into tubular and mesh-like structures (Fig. 5D). These structures in the living cell were less mobile, but showed shrinking, elongation, and contraction-like motions during observation. The localization pattern of 175 kDa myosin closely matched that of ER in cytoplasmic strands (Fig. 5B and yellow signal in Fig. 5C). In cortical regions, many signals of 175 kDa myosin (Fig. 5E) were located on the tubular networks of ER (Fig. 5E and yellow signals in Fig. 5F).

In the metaphase, some portions of ER became dispersed throughout the spindle region, but were excluded from the aligned chromosomes in the mid plane (arrows in Fig. 6A, and Supplementary Fig. S5A, B at *JXB* online). The intensity of GFP–ER signal in the spindle appeared to be higher than that in other cytoplasmic regions. During the assembly of phragmoplast, they gathered at the equatorial plane (triangles in Fig. 6C, E, G, and Supplementary Fig. S5C–F) and surrounded the daughter nuclei (arrows in Fig. 6C, E, G, and Supplementary Fig. S5D–F). ER was concentrated and formed a sharp band in the equatorial plane in mature phragmoplast (triangles in Fig. 6I and Supplementary Fig. S5F), and then diffused from this region near the end of or after mitosis (triangles in Fig. 6K, and Supplementary Fig. S5G–I). It continued to surround daughter nuclei (arrows in Fig. 6K, and Supplementary Fig. S5F–I). Signals of 175 kDa myosin (Fig. 6B, D, J, L, and lower case letters in Supplementary Fig. S5) were similar to those of GFP–ER in the spindle region, the equatorial plane in the phragmoplast, and around daughter nuclei. As described above, however, myosin signals were weaker than those of GFP–ER in the centre of the equatorial plane in the phragmoplast (long arrows in Fig. 6F and H), in which the cell plate was newly synthesized.

In contrast, the localization of organelles decorated with the anti-170 kDa myosin antibody did not change during

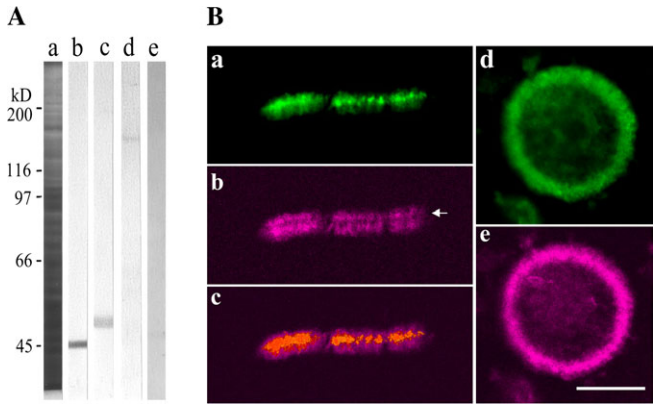


**Fig. 4.** Presence of 175 kDa myosin in isolated phragmoplasts. (A) Immunoblotting of isolated phragmoplasts was carried out using antibody against actin (b), tubulin (c), 175 kDa (d), or 170 kDa myosin heavy chain (e). Actin, tubulin, and the 175 kDa myosin, but not 170 kDa myosin, were present in the isolated phragmoplasts. (a) CBB-stained 8% SDS–polyacrylamide gel. The molecular masses of standard proteins are indicated on the left in kilodaltons. (B) Double immunofluorescence staining of isolated phragmoplasts with the antibody against 175 kDa myosin heavy chain (a and d) and RP (b and e). The 175 kDa myosin (a) was concentrated at the boundary between the opposite actin filament bundles (arrow in b) in the isolated phragmoplast. (c) Merged image of a and b. In the view from the pole, the 175 kDa myosin (d) was co-localized with the actin filament ring of the isolated phragmoplast (e). The bar represents 20 μm.

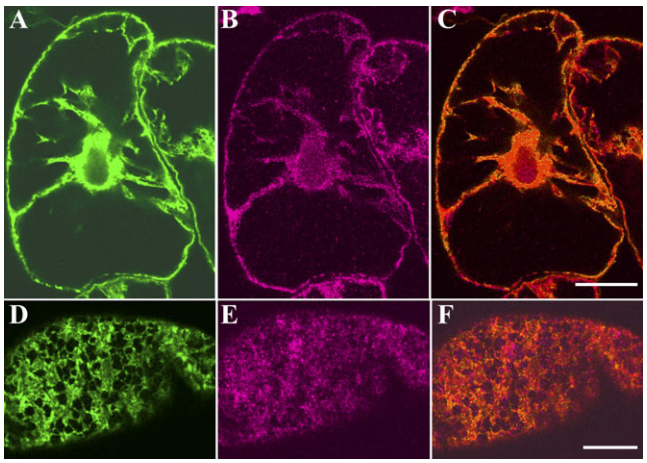


**Fig. 5.** Localization of GFP-labelled ER and the 175 kDa myosin in interphase cells. Immunofluorescence staining with the antibody against 175 kDa myosin was carried out for cells expressing GFP-labelled ER. (A and D) GFP–ER. (B and E) 175 kDa myosin. A, B, and C, and D, E, and F, were focused at nuclear and cortical regions, respectively. C and F are merged images of A and B, and D and E, respectively. The bar represents 20 μm.

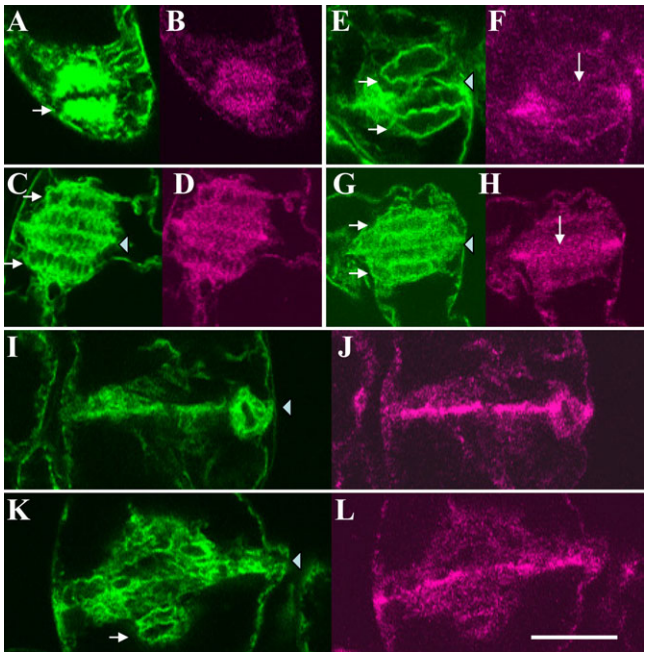


**Fig. 6.** Localization of GFP-labelled ER and the 175 kDa myosin in mitotic cells. In metaphase, some portions of ER (A) and 175 kDa myosin (B) were localized in the spindle region. Arrow indicates the position of chromosomes aligned in the mid plane. During phragmoplast assembly, ER (C, E, and G) and 175 kDa myosin (D, F, and H) were accumulated in the equatorial plane (triangles in C, E, and G) and around daughter nuclei (arrows in C, E, and G). Bright signals of ER (E and G) were also found in the centre of the equatorial plane, although weaker signals of 175 kDa myosin (long arrows in F and H) than those at the margin of the equatorial plane (F and H) were present. In the mature phragmoplast, ER (I) and 175 kDa myosin (J) were concentrated in the equatorial plane (triangle in I). During disorganization of the phragmoplast, ER (K) and the 175 kDa myosin (L) appeared to be diffused from the equatorial plane (triangle in K). The arrow in K indicates the position of daughter nuclei. The bar represents 20 μm.

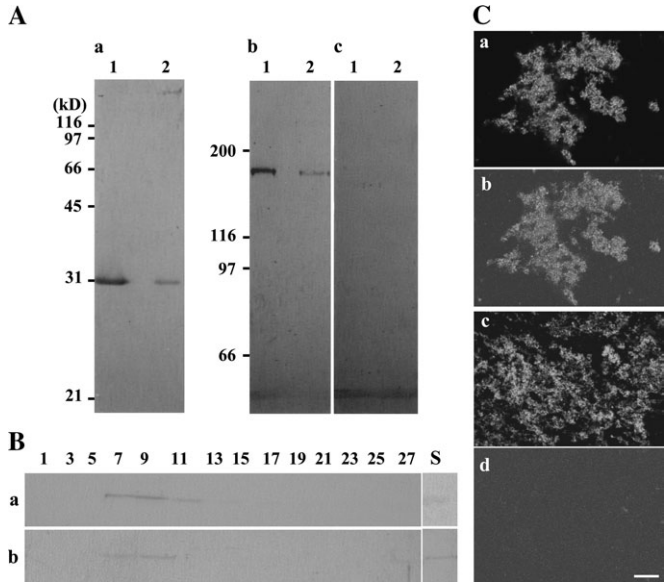


**Fig. 7.** Presence of 175 kDa myosin in the GFP–ER fraction prepared by sucrose density gradient centrifugation. (A) Immunoblotting of the 1.5 M/1.0 M (lane 1) and 1.0 M/0.6 M sucrose interface (lane 2) of discontinuous sucrose gradient centrifugation with anti-GFP antibody (a), antibody against 175 kDa myosin (b), or 170 kDa myosin heavy chain (c). The 175 kDa myosin (b) was co-distributed with GFP–ER fractions, whereas 170 kDa myosin was not detected in those fractions (c). (B) Immunoblotting of fractions obtained by continuous sucrose gradient (0.5–1.6 M) centrifugation with anti-GFP antibody (a) or antibody against 175 kDa myosin heavy chain (b). Numbers indicate the fraction numbers, and components sedimented from right (top) to left (bottom). S shows a fraction immobilized in and floating on the gradient. (C) Immunostaining of the GFP–ER fraction (a and c) recovered in the 1.5 M/1.0 M interface with anti-175 kDa myosin (b) or anti-170 kDa myosin (d). Signals of 175 kDa myosin (b) matched well with GFP–ER (a), while no signal of 170 kDa myosin (d) was observed on GFP–ER (c). The bar represents 20 μm.

mitosis; they were absent and excluded from the spindle (Supplementary Fig. S6a, b at *JXB* online) and phragmoplast (Supplementary Fig. S6c–e).

### *Association of 175 kDa myosin with isolated ER*

To evaluate further the association of ER with 175 kDa myosin, GFP–ER was isolated by sucrose density gradient ultracentrifugation from a fraction containing the microsomal fraction and cytosol. GFP–ER was recovered mainly in the interface between 1.5 M and 1.0 M sucrose (lane 1 of panel a in Fig. 7A), while a small amount of GFP–ER was found between 1.0 M and 0.6 M sucrose (lane 2 of panel a in Fig. 7A). The distribution pattern of 175 kDa myosin in the density gradient centrifugation was similar to that of GFP–ER; mainly in 1.5 M/1.0 M sucrose (panel b in Fig. 7A), while that of 170 kDa myosin was not (panel c in Fig. 7A). The distributions of both elements were also similar to each other in the continuous gradient centrifugation (Fig. 7B). However, an obvious signal of 175 kDa myosin was also detected in a fraction immobilized in and floating on the gradient (S in Fig. 7Bb), whereas there was a weaker signal of GFP in this fraction (S in Fig. 7Ba) than that in peak fractions, 7–9 in Fig. 7Ba. When the ER fraction in 1.5 M/1.0 M sucrose was immunostained with anti-myosin antibodies, signals of 175 kDa myosin (panel b in Fig. 7C) were observed on particles of GFP–ER (panel a in Fig. 7C), whereas only a few signals of 170 kDa myosin were detected (panel d in Fig. 7C) as in the case of the immunoblot analysis (panel c in Fig. 7A).

### *BDM suppresses the accumulation of GFP–ER in the equatorial plane*

To examine whether the behaviour of GFP–ER described above, such as streaming in cytoplasm, contraction-like motion in the cortical region, and accumulation in the spindle, equatorial, and pole regions, are dependent on myosin activity, a pharmacological analysis was carried out using BDM. This drug is generally and broadly used as an

inhibitor of myosin activity (see references in Yokota *et al.*, 2000) and inhibits the motile activity of myosin XI isolated biochemically from lily pollen (Tominaga *et al.*, 2000) and *Chara* (Funaki *et al.*, 2004). In interphase cells, the streaming of GFP–ER in the cytoplasmic strands and near the cortical region was stopped, and the shape change motions of the cortical GFP–ER network, especially the elongation of new ER tubes from pre-existing ER tubes or sacs, were inhibited after treatment with BDM. The suppression of streaming and ER tube elongation was also induced by treatment with the actin-depolymerizing drug latrunculin B at 2 μM, but not with the microtubule-depolymerizing drugs, oryzalin at 20 μM and propyzamide at 100 μM. However, the ER network remained and was maintained even with the treatment with BDM or latrunculin B.

When cells synchronized by the two-step procedure were treated with BDM, the cell cycle progressed similarly to control cells. Figure 8A shows the percentage of cells in each mitotic stage at 90 min after releasing cells from propyzamide and then treating them with BDM. The percentage of cells treated with BDM (black bars in Fig. 8A) in each mitotic stage was similar to that of control cells (white bars in Fig. 8A), and cell plate formation was not significantly different between BDM-treated and control cells (compare Fig. 9c with d). Furthermore, GFP–ER in treated cells (Fig. 9B) was present in the spindle region at a similar level to that in control cells (Fig. 9A). Since the metaphase started soon after releasing cells from propyzamide, the treatment period with BDM was very short. Hence, it was not confirmed whether the accumulation of ER in the spindle was dependent on myosin activities.

The width of ER between daughter nuclei in treated cells did not become narrow during mitosis (Fig. 9D). Also, in optical sections, GFP–ER seemed to be distributed widely between daughter nuclei in the treated cells (Fig. 9G–I), whereas it appeared to be in a line in the equatorial plane in control cells (Fig. 9J). Figure 8B shows the statistical analysis of ER width between daughter nuclei in mid to late telophase. In control cells, ER present in the spindle region accumulated in the equatorial plane (Fig. 9C, J) as described above, and, as a result, the width of ER in mid to late telophase was narrow, with an average width of ~2 μm (white bars in Fig. 8B). In contrast, the average width of ER in treated cells was ~10–16 μm (black bars in Fig. 8B). In addition, the intensity of GFP–ER signals around daughter nuclei in the treated cells was apparently weaker than that in control cells (compare Fig. 9C with D, or Fig. 9J with G–I). These results indicated the suppression of accumulation of ER both in the equatorial plane and around daughter nuclei by BDM. Signals of 175 kDa myosin (Fig. 9k, l) were similar to those of GFP–ER (Fig. 9K, L) around daughter nuclei and not accumulated in the equatorial region of the phragmoplast in BDM-treated cells.

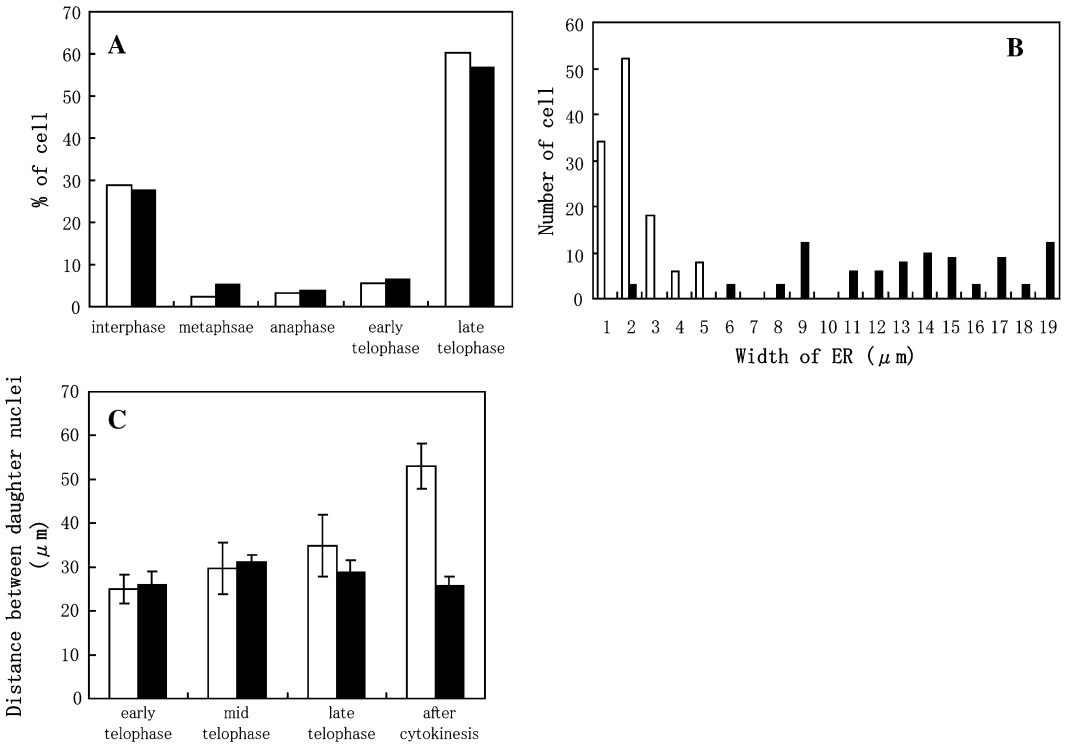


**Fig. 8.** Effects of BDM on the progression of the cell cycle (A), width of GFP–ER in phragmoplasts (B), and distance between daughter nuclei during and after mitosis (C). After releasing cells from propyzamide, they were treated (black bars) or not with 50 mM BDM (white bars). After 90 min, cells in each stage were counted. Progression of the cell cycle was not suppressed by BDM treatment (A). The width of the ER between daughter nuclei of untreated cells (white bars in B) in mid to late telophase was narrow; however, it was broad in cells treated with BDM (black bars in B). Furthermore, the distance between daughter nuclei of BDM-treated cells was not increased particularly even after mitosis (C). Averages are shown with the SD.

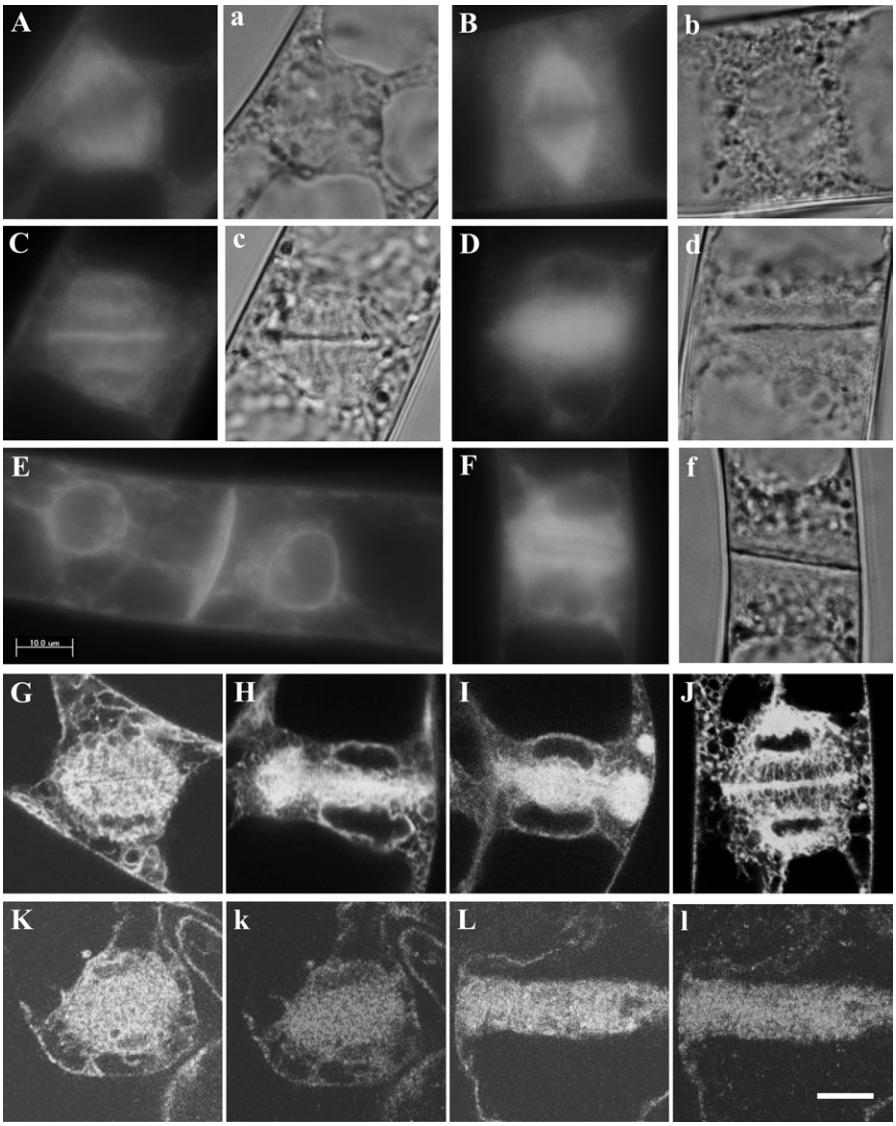


**Fig. 9.** Suppression of ER accumulation in the equatorial plane and around daughter nuclei, and of positioning of daughter nuclei in the centre of daughter cells by BDM, and localization of 175 kDa myosin in BDM-treated cells. GFP–ER (upper case letters), differential interference contrast images (a, b, c, and f), and signals of 175 kDa myosin (k and l) are shown. After releasing cells from propyzamide, they were treated (B, D, F, G, H, I, K, L, k, and l) or not with 50 mM BDM (A, C, E, and J). The accumulation of GFP–ER in the spindle region was not suppressed by treatment with BDM (B), perhaps because spindle formation began soon after release from propyzamide. In mid telophase, GFP–ER accumulated in the equatorial plane of phragmoplast and around daughter nuclei in cells without BDM treatment (C and J). The cell plate was assembled between daughter nuclei (c). However, accumulation of GFP–ER in the equatorial planes and around daughter nuclei was suppressed by the treatment with BDM (D), although the cell plate was assembled (d). The suppression of those events was confirmed by observation using a laser scanning microscope (G, H and I). After mitosis of control cells, daughter nuclei moved to the centre of each daughter cell (E), whereas they did not in BDM-treated cells (F). The 175 kDa myosin (k and l) in the cells treated with BDM was in a similar localization pattern to GFP–ER (K and L). Bars represent 10 μm.

Although the organization of microtubules in the phragmoplasts of BDM-treated cells (Supplementary Fig. S7a–c at *JXB* online) appeared to be similar to that of control cells, two types of actin filament organization in this region were observed at a similar frequency. One type (Supplementary Fig. S8a, b) was similar to that observed in control cells. In the second type (Supplementary Fig. S8c, d), the boundary region of opposite actin filament bundles became clear (arrows in Supplementary Fig. S8), perhaps because of the expansion of this region. However, the accumulation of GFP–ER in the equatorial planes of phragmoplasts was suppressed in both types of cells (Supplementary Fig. S8A, B for the former type, and S8C, D for the latter type).

The distance between daughter nuclei in each late mitotic stage was different between treated (black bars in Fig. 8C) and control cells (white bars in Fig. 8C). During the progression of mitosis in control cells, the distance between daughter nuclei was gradually increased and then daughter nuclei were positioned near the centre of each daughter cell after mitosis (Fig. 9E). However, that of treated cells was

slightly decreased from late telophase after mitosis, and, as a result, daughter nuclei were positioned near the newly synthesized cell wall (Fig. 9F).

### *ER and 175 kDa myosin gather at PPB regions*

Zachariadis *et al.* (2001) found that a part of the ER is arrayed in a ring-like structure at the site of the PPB in root tip cells of *Pinus brutia*. The localization of 175 kDa myosin correlated with that of ER as described above, suggesting the possibility that the 175 kDa myosin together with GFP–ER gathers at PPB sites during pre-prophase in BY-2 cells. Finally, to confirm this possibility, the cells were synchronized by a one-step procedure. Although the mitotic index was low, <40%, this procedure allowed the effective observation of cells having a PPB. In the cortical site where the PPB was arranged (triangle in Fig. 10a), cortical actin filaments were aligned in parallel more or less with microtubules in the PPB (Fig. 10A). Some parts of the 175 kDa myosin preferentially gathered at the PPB region. In premature PPBs in which microtubule bundles were broad (triangles in Fig. 10b, and Supplementary Fig. S9a–d at *JXB* online), the 175 kDa myosin also became localized broadly in this site (Fig. 10B, and Supplementary Fig. S9A–D). When microtubules were tightly packed in the mature PPB (triangles in Fig. 10c and Supplementary Fig. S9e), a line-like structure (Fig. 10C and Supplementary Fig. S9E) of 175 kDa myosin signals was found in this region. As reported by Zachariadis *et al.* (2001), some parts of GFP–ER gathered at the PPB site (Fig. 10D, and Supplementary Fig. S10A–C) and formed a sharp line in mature PPB (Fig. 10E), with which the 175 kDa myosin was co-localized (triangles in Fig. 10e, and Supplementary Fig. S11d, e). In the premature PPB, this myosin (triangles in Supplementary Fig. S11a–c) was also co-localized with GFP–ER (Supplementary Fig. S11A–C).

When cells were synchronized by the one-step procedure and were treated with BDM after they were released from aphidicolin, the cell cycle ceased before pre-prophase because of the long period of treatment, >2 h, with BDM. Hence it was not possible to examine whether myosin activity is required for the accumulation of ER in the PPB regions.

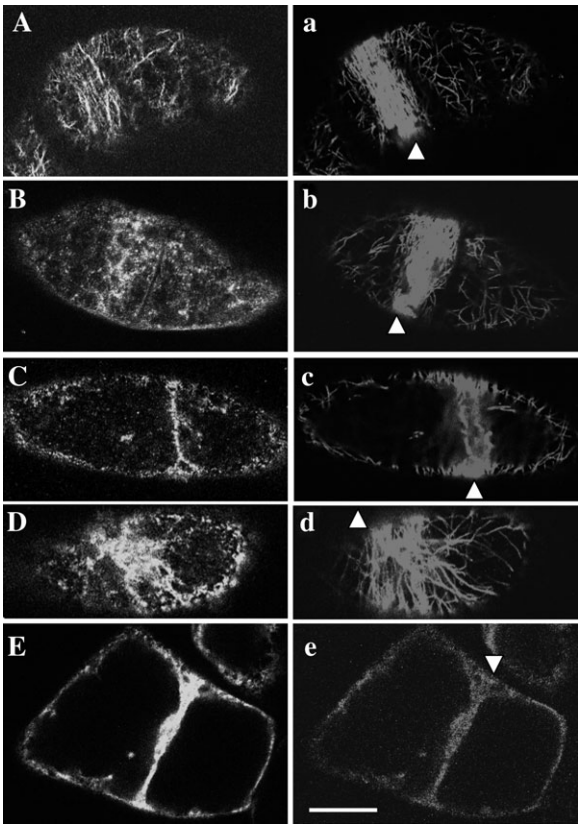


**Fig. 10.** Localization of microtubule, actin filament, 175 kDa myosin, and GFP–ER in the PPB region. (A and a) Distribution of actin filaments stained with Bodipy FL phallacidin and microtubules immunostained with anti-tubulin antibody, respectively. Actin filaments (A) with more or less parallel orientation with microtubules (triangle in a) were arrayed in the PPB region. (B and C, and b and c) Distribution of 175 kDa myosin and microtubules, respectively. In a premature PPB region, in which microtubules were loosely packed (triangle in b), the 175 kDa myosin was widely distributed (B). On the other hand, 175 kDa myosin was concentrated in a sharp line (C) beneath the mature and tightly packed microtubule bundle (triangle in c). (D and d) Distribution of GFP–ER and microtubules, respectively. In the premature PPB region (triangle in d), GFP–ER was widely distributed (D). (E and e) Distribution of GFP–ER and 175 kDa myosin, respectively, in the mature PPB region. Both components became concentrated and formed a line in this region (triangle in e). The bar represents 20 μm.

## Discussion

The 175 kDa myosin has been isolated biochemically from BY-2 cells and suggested to be involved in cytoplasmic streaming based on analysis of its sliding activity *in vitro* (Yokota *et al.*, 1999). In the present study, it was shown that the 175 kDa myosin was localized throughout cytoplasm as fine dots and accumulated in the PPB, spindle, phragmoplast and around daughter nuclei during mitosis. Furthermore, this localization pattern was similar to that of GFP–ER.

### *The translocation of ER in the cytoplasm*

In interphase cells, GFP–ER was localized in both the cortical region and cytoplasmic strands (Fig. 5), where it was translocated with an average velocity ranging from 4 μm $s^{-1}$ to 9 μm $s^{-1}$. In the GFP–ER fraction isolated by the sucrose density gradient ultracentrifugation procedure, the 175 kDa myosin was detected and located on the GFP–ER vesicles (Fig. 7). Taken together with the evidence showing the co-localization of 175 kDa myosin and GFP–ER in the cytoplasm, these results indicated that this myosin is associated with ER. It has been reported that this myosin was able to translocate RP-labelled F-actin at an average velocity of ~9 μm $s^{-1}$ in an *in vitro* motility assay (Yokota *et al.*, 1999). This sliding velocity was comparable with the velocity of GFP–ER in BY-2 cells. Hence, it was

suggested that the 175 kDa myosin is one of the molecular motors for translocating ER in the cytoplasm.

### *The ER network in the cortical region*

In the cortical region, GFP–ER was arranged into tubular and mesh-like structures (Fig. 5) that were not translocated but exhibited shape changes. Some portions, but not all, of 175 kDa myosin were located on the GFP–ER meshwork (Fig. 5). In epidermal cells of onion bulb scales (Quader and Schnepf, 1986; Quader, 1990; Knebel *et al.*, 1990) and mesophyll cells of *Vallisneria* (Liebe and Menzel, 1995), peripheral tubular and lamellar ER in the cortical region is less motile but the tubular ER preferentially shows shape changes, such as new tube elongation from a pre-existing tube and sac. From the pharmacological studies using actin-depolymerizing drugs, the streaming of ER not only in cytoplasm but also in the cortical region is shown to be mediated by actin filaments. The present study showed that BDM also inhibited the tube elongation of cortical ER in BY-2 cells, like the actin-depolymerizing drug latrunculin B, whereas microtubule-depolymerizing drugs did not. These results supported the involvement of the actin cytoskeleton in the shape change of the cortical ER in higher plant cells. Hence, it was possible to consider that 175 kDa myosin was also responsible for this event. On the other hand, Golomb *et al.* (2008) recently showed the co-localization of fine dots decorated with myosin VIII with the cortical ER network in tobacco, *Nicotiana benthamiana*, cells, raising another possibility that this myosin class is involved in cortical ER dynamics. In contrast to plant cells, the dynamics of the cortical ER network in animal cells has been indicated to depend mainly on the microtubule (Voeltz *et al.*, 2002). However, Dreier and Rapoport (2000) demonstrated that isolated ER vesicles from *Xenopus* eggs formed mesh-like structures *in vitro*, and the cytoskeleton was not involved in this event. Furthermore, they showed recently that reticulon family proteins play a crucial role in the formation of the cortical ER network, especially the elongation of tubular structure of ER (Voeltz *et al.*, 2006). These results raised the possibility that the actin–myosin system containing 175 kDa myosin or myosin VIII did not contribute to the shape change of the cortical ER network. Further study is needed to elucidate this possibility.

### *The 175 kDa myosin and ER in the PPB and spindle regions*

In pre-prophase BY-2 cells, some parts of the ER accumulated and became concentrated in the area of the PPB (Fig. 10) as reported for maize root cells (Zachariadis *et al.*, 2001), although the mechanism of the accumulation and the role of ER in this region remain to be resolved. In many cases, actin filament bundles are arranged with a parallel orientation of microtubules in this region (Mineyuki, 1999). In BY-2 cells, this was also reported by Kakimoto and Shibaoka (1987) and in the present study (Fig. 10). The 175 kDa myosin was co-localized with concentrated ER in the PPB region. Hence, it was assumed that the 175 kDa myosin contributes to the transport and reorganization of ER in the PPB region along rearranged actin filaments in parallel orientation with microtubules in this region.

In metaphase, some, but not all, of the ER and 175 kDa myosin gathered in the spindle region. They were also located in the remaining cytoplasm, as is the case in interphase cells. However, the intensity of their signals in the spindle region appeared to be higher than those in other regions (Fig. 6A), suggesting that ER preferentially accumulates in this region before or during metaphase. For this purpose, the sliding activity of 175 kDa myosin should be suppressed at this stage, because actin filaments continued to be present in cytoplasmic strands and around the spindle region (Schmit, 2000; Sano *et al.*, 2005). The velocity of ER translocation in cytoplasm in mitotic cells was reduced to about half of that in interphase cells. It has been reported that cytoplasmic streaming in the nuclear region is suppressed during mitosis (Mineyuki *et al.*, 1984). To date, $Ca^{2+}$ is considered to be one of the signals for such suppression, because the sliding activity of 175 kDa myosin *in vitro* is inhibited by $Ca^{2+}$ (Yokota *et al.*, 1999; Tominaga *et al.*, 2004).

### *The role of actin filament bundle in the phragmoplast*

During anaphase to telophase, the 175 kDa myosin and ER dispersed in the spindle region were accumulated in the equatorial plane of the phragmoplast and around daughter nuclei (Fig. 6). In the phragmoplast, the polarity of the actin filaments is uniform in each opposite bundle and their barbed ends are pointed towards the centre of the equatorial plane (Kakimoto and Shibaoka, 1988). The 175 kDa myosin moves along F-actin *in vitro* from its pointed to its barbed filament end (Tominaga *et al.*, 2003). Hence, the polarity of actin bundles in phragmoplasts should favour myosin translocating the cargo to the equatorial plane. Furthermore, the accumulation and concentration of GFP–ER in the equatorial plane was blocked by treatment with BDM (Figs 8, 9). Recently, Higaki *et al.* (2008) reported the suppression of GFP–ER accumulation in the equatorial plane of phragmoplasts in BY-2 cell by an actin-depolymerizing drug bistheonellide A, and indicated the role of actin filament bundles in the transport of ER to this region. The role of actin filament bundles in the phragmoplast has been less clear than that of microtubule bundles. The present study further suggested that actin filament bundles play a role as tracks along which 175 kDa myosin translocates ER to the equatorial plane. Higaki *et al.* (2008) also showed that the movement of endosomes around the expanding cell plate edges is suppressed by treatment with BDM or bistheonellide A, suggesting that the actin filament bundles in the phragmoplasts are also responsible for the movement of endosomes. At present, it is not known that myosin XI including 175 kDa myosin is involved in their movement. Myosin VIII was found to be co-localized on endocytotic vesicles (Golomb *et al.*, 2008), raising the possibility that this myosin is involved in the movement of endosomes, instead of myosin XI.

In BDM-treated cells, the organization of actin filament bundles in the phragmoplasts was altered (Supplementary Fig. S8 at *JXB* online). However, in BDM-treated cells having similar actin organization to control cells in this region, the GFP–ER accumulation in the equatorial planes was suppressed. Hence, it was likely that the suppression of GFP–ER accumulation was due to the inhibition of myosin activity. Furthermore, the possibility is considered that the organization of the actin filament bundle in the phragmoplast is arranged or maintained by myosin.

One function of ER in the phragmoplast is considered to be control of the $Ca^{2+}$ concentration, which is expected to be higher than in other parts of the cell (Hepler, 1989; Staehelin and Hepler, 1996), although the exact concentration of $Ca^{2+}$ in the phragmoplast, especially in its equatorial plane, has not yet been estimated. As described above, $Ca^{2+}$ at micromolar concentrations suppresses the sliding activity of 175 kDa myosin (Yokota *et al.*, 1999; Tominaga *et al.*, 2004). If the motile activity of 175 kDa myosin is exerted fully in the phragmoplast, the accumulation of ER in the equatorial plane would be over in a few seconds. However, it takes several minutes for accumulation of ER in the equatorial plane in the cell (Supplementary Fig. S12 at *JXB* online). Hence, it is plausible that the activity of 175 kDa myosin is regulated in the phragmoplast especially by $Ca^{2+}$. The 175 kDa myosin was concentrated at the boundary between the opposite actin filament bundles (Fig. 3), where few actin filaments are found (Staehelin and Hepler, 1996). This was further supported by an examination of 175 kDa myosin and actin filament distribution in isolated phragmoplasts (Fig. 4). Therefore, instead of actin–myosin interaction, it appears likely that another mechanism exists for tethering ER on the equatorial plane of the phragmoplast.

### *The role of ER in the cell plate*

Molchan *et al.* (2002) have reported that a wavy cell plate was formed in *Tradescantia* stamen hair cells treated with BDM. In the present study, the cell plate was also formed in BY-cells treated with BDM and its morphology appeared not to be significantly different from that of control cells, although the accumulation of ER in the equatorial plane was suppressed (Figs 8, 9). The formation of a cell plate in BY-2 cells treated with BDM has also been shown by Higaki *et al.* (2006). The present studies indicated that the formation of a cell plate could occur even when the position and organization of ER in phragmoplasts were disturbed, suggesting that ER is not an essential component for the formation of the cell plate. On the other hand, it has been revealed that ER is kept and trapped in newly synthesized cell plates to construct plasmodesmata in multicellular tissues (Hawes *et al.*, 1981; Hepler, 1982). Therefore, the translocation of ER to the equatorial plane of the phragmoplast was considered to be a crucial event for constructing proper plasmodesmata, and myosin XI was responsible for this event. Another type of plant myosin, myosin VIII, has been reported to be accumulated in the cell plate and be incorporated into plasmodesmata (Blauska *et al.*, 2001; Volkmann *et al.*, 2003). Although it has not been shown which structure(s) myosin VIII is associated with or what the role of this myosin is in the cell plate, two types of myosins with different roles were revealed to be present in the phragmoplast and cell plate; myosin XI translocating ER and myosin VIII incorporated into plasmodesmata.

### *The 175 kDa myosin around daughter nuclei*

During mitosis, ER and 175 kDa myosin were also accumulated around daughter nuclei (Fig. 6). In BDM-treated cells, the intensity of GFP–ER around daughter nuclei was obviously weaker than that of control cells (Fig. 9). From these results, it was plausible to consider that the accumulation of ER around daughter nuclei was also dependent on 175 kDa myosin activity. The role of 175 kDa myosin remaining around the daughter nuclei had not been clear. Some possibilities were put forward; for example, the precise inheritance of ER by daughter cells (Sheahan *et al.*, 2004) and its involvement in the reformation of the nuclear envelope after ER fusion. The ER retention signal peptide, HDEL, transduced in the cells used in the present study is incorporated into nuclear envelopes (Napier *et al.*, 1992), perhaps due to the fusion of ER with them. Therefore, it is possible that the 175 kDa myosin might be associated with not only ER, but also with the nuclear envelope of daughter nuclei. Molchan *et al.* (2002) showed that *Tradescantia* stamen hair cells treated with BDM displayed thicker phragmoplasts than control cells, and supposed that nuclear envelope-associated myosin anchors and connects the telophase daughter nuclei with the phragmoplast by pulling them along actin filaments. This hypothesis is attractive for speculating on the function of 175 kDa myosin around the daughter chromosomes and nuclei. BDM has been reported to alter cytoplasmic structures, such as cytoplasmic strands in BY-2 cells (Higaki *et al.*, 2006) and transvacuolar strands in root hair cells of *Limunobium* (Yokota *et al.*, 2000). In the present study, the change of organization of actin filament bundle in the phragmoplast produced by this drug was also shown (Supplementary Fig. S8 at *JXB* online). However, in the present study it was confirmed whether or not the organization of actin filament in other regions is altered by BDM in late telophase. Hence, the possibility that the positioning of daughter nuclei in this stage and after mitosis is affected due to the alteration of actin filament or cytoplasmic organization, instead of the suppression of 175 kDa myosin activity around daughter nuclei, is not ruled out.

### *The 175 kDa myosin isolated biochemically*

The 175 kDa myosin has been isolated biochemically from the cytosol of BY-2 protoplasts by breakage with a motor-driven homogenizer (Yokota *et al.*, 1999). In the present study, this myosin was detected in the fraction immobilized

in and floating on the sucrose gradient after the centrifugation (Fig. 7), as well as in fractions also containing GFP–ER. Protoplasts were also broken by a hand-operated homogenizer. Hence, some portions of this myosin associated with ER may be released by the shear stress of homogenization in the protoplast breakage step, and the released form may have been detected in the former fraction and isolated biochemically in previous work. However, another possibility is also considered that free 175 kDa myosin, which is not associated with ER, is present and isolated.

The present study showed the association of 175 kDa myosin with ER using an antibody against the whole heavy chain molecule. Therefore, it is not possible to rule out the possibility that this antibody also recognizes other types of myosin XI as yet unidentified in BY-2 cells. As described in the Introduction, myosin XI is found to be associated with the Golgi, peroxisomes, mitochondria, and plastids, and is suggested to be responsible for the translocation and movement of these organelles. The present study showed the involvement of myosin XI in the translocation of ER in higher plant cells.

## Supplementary data

Supplementary data are available at *JXB* online.

**Figure S1.** Immunoblotting of crude extract of BY-2 cells with an antibody against 175 kDa myosin heavy chain.

**Figure S2.** Localization of 175 kDa myosin and microtubule in mitotic BY-2 cells.

**Figure S3.** Localization of 175 kDa myosin and actin filament in mitotic BY-2 cells.

**Figure S4.** Localization of 175 kDa myosin in isolated phragmoplasts.

**Figure S5.** Positional relationship of GFP–ER with 175 kDa myosin in mitotic BY-2 cells.

**Figure S6.** Localization of 170 kDa myosin in mitotic BY-2 cells.

**Figure S7.** Organization of microtubule in phragmoplasts in BDM-treated BY-2 cells.

**Figure S8.** Organization of actin filament in phragmoplasts in BDM-treated BY-2 cells.

**Figure S9.** Localization of 175 kDa myosin in the PPB region.

**Figure S10.** Localization of GFP–ER in the PPB region.

**Figure S11.** Positional relationship of GFP–ER with 175 kDa myosin in the PPB region.

**Figure S12.** Time course of GFP–ER accumulation in the equatorial plane of the phragmoplast in a living BY-2 cell.

## Acknowledgements

We thank the National Live Stock Breeding Center Hyogo Station for the gift of chicken breast muscle. This work was supported by Grant-in-Aid for Special Research on Priority Areas (grant no. 17051026) and Grant-in-Aid for Special Research C (grant no. 175700433).

## References

**Avisar D, Prokhnevsky AI, Makarova KS, Koonin EV, Dolja VV.** 2008. Myosin XI-K is required for rapid trafficking of Golgi stacks, peroxisomes, and mitochondria in leaf cells of *Nicotiana benthamiana*. *Plant Physiology* **146,** 1098–1108.

**Baluska F, Cvrckova F, Kendrick-Jones J, Volkmann D.** 2001. Sink plasmodesmata as gateways for phloem unloading. Myosin VIII and calreticulin as molecular determinants of sink strength? *Plant Physiology* **126,** 39–46.

**Boevink P, Oparka K, Cruz SS, Martin B, Betteridge A, Hawes C.** 1998. Stacks on tracks: the plant Golgi apparatus traffics on an actin/ER network. *The Plant Journal* **15,** 441–447.

**Collings DA, Harper JDI, Marc J, Overall RL, Mullen RT.** 2002. Life in the fast lane: actin-based motility of plant peroxisomes. *Canadian Journal of Botany* **80,** 430–441.

**Collings DA, Harper JDI, Vaughn KC.** 2003. The association of peroxisomes with developing cell plate in dividing onion root cells depends on actin microfilaments and myosin. *Planta* **218,** 204–216.

**Denecke J, Carlsson LE, Vidal S, Hoglund A-S, Ek B, van Zeiji MJ, Sinjorgo KMC, Palva ET.** 1995. The tobacco homolog of mammalian calreticulin is present in protein complexes *in vivo*. *The Plant Cell* **7,** 391–406.

**Dong JG, Satoh S, Fujii T.** 1988. Variation in endoplasmic reticulum-associated glycoproteins of carrot cells cultured *in vitro*. *Planta* **173,** 419–423.

**Dreier L, Rapoport TA.** 2000. *In vitro* formation of the endoplasmic reticulum occurs independently of microtubules by a controlled fusion reaction. *Journal of Cell Biology* **148,** 883–898.

**Foth BJ, Goedecke MC, Solsati D.** 2006. New insights into myosin evolution and classification. *Proceedings of the National Academy of Sciences, USA* **103,** 3681–3686.

**Frank DJ, Noguchi T, Miller KG.** 2004. Myosin VI: a structural role in actin organization important for protein and organelle localization and trafficking. *Current Opinion in Cell Biology* **16,** 189–194.

**Funaki K, Nagata A, Akimoto Y, Shimada K, Ito K, Yamamoto K.** 2004. The motility of Chara corallina myosin was inhibited reversibly by 2,3-butanedione monoxime (BDM). *Plant and Cell Physiology* **45,** 1342–1345.

**Golomb L, Abu-Abied M, Belausov E, Sadot E.** 2008. Different subcellular localization and functions of Arabidopsis myosin VIII. *BMC Plant Biology* **8,** 1–13.

**Hachikubo Y, Ito K, Schiefelbein J, Manstein D, Yamamoto K.** 2007. Enzymatic activity and motility of recombinant Arabidopsis myosin XI, MYA1. *Plant and Cell Physiology* **48,** 886–891.

**Hashimoto K, Igarashi H, Mano S, Nishimura M, Shimmen T, Yokota E.** 2005. Peroxisomal localization of a myosin XI isoform in Arabidopsis thaliana. *Plant and Cell Physiology* **46,** 782–789.

**Hawes CR, Juniper BE, Horne JC.** 1981. Low and high voltage electron microscopy of mitosis and cytokinesis in maize roots. *Planta* **152,** 397–407.

**Hepler PK.** 1980. Membranes in the mitotic apparatus of barley cells. *Journal of Cell Biology* **86,** 490–499.

**Hepler PK.** 1982. Endoplasmic reticulum in the formation of the cell plate and plasmodesmata. *Protoplasma* **111,** 121–133.

**Hepler PK.** 1989. Calcium transients during mitosis: observation in flux. *Journal of Cell Biology* **109,** 2567–2573.

**Higaki T, Kutsuna N, Okubo E, Sano T, Hasezawa S.** 2006. Actin microfilaments regulate vacuolar structures and dynamics: dual observation of actin microfilaments and vacuolar membrane in living tobacco BY-2 cells. *Plant and Cell Physiology* **47,** 839–852.

**Higaki T, Kutsuna N, Sano T, Hasezawa S.** 2008. Quantitative analysis of changes in actin microfilament contribution to cell plate development in plant cytokinesis. *BMC Plant Biology* **8,** 1–15.

**Jedd G, Chua N-H.** 2002. Visualization of peroxisomes in living plant cells reveals acto-myosin-dependent cytoplasmic streaming and peroxisome budding. *Plant and Cell Physiology* **43,** 384–392.

**Kakimoto T, Shibaoka H.** 1987. Actin filaments and microtubules in the preprophase band and phragmoplast of tobacco cells. *Protoplasma* **140,** 151–156.

**Kakimoto T, Shibaoka H.** 1988. Cytoskeletal ultrastructure of phragmoplast–nuclei complexes isolated from cultured tobacco cells. *Protoplasma Supplement* **2,** 95–103.

**Kinkema M, Schiefelbein J.** 1994. A myosin from a higher plant has structural similarities to class V myosins. *Journal of Molecular Biology* **239,** 591–597.

**Kinkema M, Wang H, Schiefelbein J.** 1994. Molecular analysis of the myosin gene family in Arabidopsis thaliana. *Plant Molecular Biology* **26,** 1139–1153.

**Knebel W, Quader H, Schnepf E.** 1990. Mobile and immobile endoplasmic reticulum in onion bulb spidermis cells: short- and long-term observations with a confocal laser scanning microscope. *European Journal of Cell Biology* **52,** 328–340.

**Knight AE, Kendrick-Jones J.** 1993. A myosin-like protein from a higher plant. *Journal of Molecular Biology* **231,** 148–154.

**Korn ED.** 2000. Coevolution of head, neck, and tail domains of myosin heavy chains. *Proceedings of the National Academy of Sciences, USA* **97,** 12559–12564.

**Kwok EY, Hanson MR.** 2003. Microfilaments and microtubules control the morphology and movement of non-green plastids and stromules in Nicotiana tabacum. *The Plant Journal* **35,** 16–26.

**Laemmli UK.** 1970. Cleavage of structural proteins during the assembly of the head of bacteriophage T4. *Nature* **227,** 680–685.

**Li J-F, Nebenfuhr A.** 2007. Organelle targeting of myosin XI is mediated by two globular tail subdomains with separate cargo binding sites. *Journal of Biological Chemistry* **282,** 20593–20602.

**Liebe S, Menzel D.** 1995. Actomyosin-based motility of endoplasmic reticulum and chloroplasts in *Vallisneria* mesophyll cells. *Biology of the Cell* **8,** 207–222.

**Liu L, Zhou J, Pesacreta TC.** 2001. Maize myosins: diversity, localization and function. *Cell Motility and the Cytoskeleton* **48,** 130–148.

**Logan DC, Leaver CJ.** 2000. Mitochondria-targeted GFP highlights the heterogeneity of mitochondrial shape, size and movement within living plant cells. *Journal of Experimental Botany* **346,** 865–871.

**Mano S, Nakamori C, Hayashi M, Kato A, Kondo M, Nishimura M.** 2002. Distribution and characterization of peroxisomes in Arabidopsis by visualization with GFP: dynamic morphology and actin-dependent movement. *Plant and Cell Physiology* **43,** 331–341.

**Mathur J, Mathur N, Hulskamp M.** 2002. Simultaneous visualization of peroxisomes and cytoskeletal elements reveals actin and not microtubule-based peroxisome motility in plants. *Plant Physiology* **128,** 1031–1045.

**Mermall V, Post PL, Mooseker MS.** 1998. Unconventional myosins in cell movement, membrane traffic, and signal transduction. *Science* **279,** 527–533.

**Mineyuki Y.** 1999. The preprophase band of microtubules: its function as a cytokinetic apparatus in higher plants. *International Review of Cytology* **187,** 1–49.

**Mineyuki Y, Takagi M, Furuya M.** 1984. Changes in organelle movement in the nuclear region during the cell cycle of *Adiantum* protonemata. *Plant and Cell Physiology* **25,** 297–308.

**Mitsuhasi N, Shimada T, Mano S, Nishimura M, Hara-Nishimura I.** 2000. Characterization of organelles in the vacuolar-sorting pathway by visualization with GFP in tobacco BY-2 cells. *Plant and Cell Physiology* **41,** 993–1001.

**Molchan TM, Valster AH, Hepler PK.** 2002. Actomyosin promotes cell plate alignment and late lateral expansion in *Tradescantia* stamen hair cells. *Planta* **214,** 683–693.

**Nagata T, Okada K, Takebe I, Matsui C.** 1981. Delivery of tobacco mosaic virus RNA into plant protoplasts mediated by reverse-phase evaporation vesicle (liposomes). *Molecular and General Genetics* **184,** 161–165.

**Napier RM, Fowke LC, Hawes C, Lewis M, Pelham HRB.** 1992. Immunological evidence that plants use both HDEL and KDEL for targeting proteins to the endoplasmic reticulum. *Journal of Cell Science* **102,** 261–271.

**Nebenfuhr A, Frohlick JA, Staehelin LA.** 2000. Redistribution of golgi stacks and other organelles during mitosis and cytokinesis in plant cells. *Plant Physiology* **124,** 135–151.

**Nebenfuhr A, Gallagher L, Dunahay TG, Frohlick JA, Mazurkiewicz AM, Staehelin LA.** 1999. Stop-go movements of plant golgi stacks are mediated by the acto-myosin system. *Plant Physiology* **121,** 1127–1141.

**Paves H, Truve E.** 2007. Myosin inhibitors block accumulation movement of chloroplasts in *Arabidopsis thaliana* leaf cells. *Protoplasma* **230,** 165–169.

**Peremyslov VV, Prokhnevsky AI, Avisar D, Dolja VV.** 2008. Two class XI myosins function in organelle trafficking and root hair development in Arabidopsis. *Plant Physiology* **146,** 1109–1116.

**Quader H.** 1990. Formation and disintegration of cisternae of the endoplasmic reticulum visualized in live cells by conventional fluorescence and confocal laser scanning microscopy: evidence for the involvement of calcium and cytoskeleton. *Protoplasma* **155,** 166–175.

**Quader H, Schnepf E.** 1986. Endoplasmic reticulum and cytoplasmic streaming: fluorescence microscopical observations in adaxial epidermis cells of onion bulb scales. *Protoplasma* **131,** 250–252.

**Reck-Peterson SL, Provance DW Jr, Mooseker MS, Mercer JA.** 2000. Class V myosins. *Biochimica et Biophysica Acta* **1496,** 36–51.

**Reddy ASN.** 2001. Molecular motors and their functions in plants. *International Review of Cytology* **204,** 97–178.

**Reddy ASN, Day IS.** 2001. Analysis of the myosin encoded in the recently completed Arabidopsis thaliana genome sequence. *Genome Biology* **2,** 0024.1–0024.17.

**Reichelt S, Kendrick-Jones J.** 2000. Myosins. In: Staiger CJ, Baluska F, Volkmann D, Barlow PW, eds. *Actin: dynamic framework for multiple plant cell functions*. Dordrecht: Kluwer Academic Publishers, 29–44.

**Reisen D, Hanson MR.** 2006. Association of six YFP–myosin XI-tail fusions with mobile plant cell organelles. *BMC Plant Biology* **7,** 1–17.

**Romagnoli S, Cai G, Faleri C, Yokota E, Shimmen T, Cresti M.** 2007. Microtubule- and actin filament-dependent motors are distributed on pollen tube mitochondria and contribute differently to their movement. *Plant and Cell Physiology* **48,** 345–361.

**Sano T, Higaki T, Oda Y, Hayashi T, Hasezawa S.** 2005. Appearance of actin microfilament 'twin peaks' in mitosis and their function in cell plate formation, as visualized in tobacco BY-2 cells expressing GFP–fimbrin. *The Plant Journal* **44,** 595–605.

**Schmit A-C.** 2000. Actin during mitosis and cytokinesis. Structure and function of the F-actin cytoskeleton. In: Staiger CJ, Baluska F, Volkmann D, Barlow PW, eds. *Actin: dynamic framework for multiple plant cell functions*. Dordrecht: Kluwer Academic Publishers, 437–456.

**Shimmen T, Yokota E.** 2004. Cytoplasmic streaming in plants. *Current Opinion in Cell Biology* **16,** 68–72.

**Sheahan M, Rose RJ, McCurdy DW.** 2004. Organelle inheritance in plant cell division: the actin cytoskeleton is required for unbiased inheritance of chloroplasts, mitochondria and endoplasmic reticulum in dividing protoplasts. *The Plant Journal* **37,** 379–390.

**Staehelin LA, Hepler PK.** 1996. Cytokinesis in higher plants. *Cell* **84,** 821–824.

**Tominaga M, Kojima H, Yokota E, Orii H, Nakamori R, Katayama E, Anson M, Shimmen T, Oiwa K.** 2003. Higher plant myosin XI moves processively on actin with 35 nm steps at high velocity. *EMBO Journal* **22,** 1263–1272.

**Tominaga M, Yokota E, Nakamori R, Shimmen T, Oiwa K.** 2004. Calcium regulation mechanism of higher plant myosin XI responsible for cytoplasmic streaming. *Plant and Cell Physiology* **45,** (Suppl), s115.

**Tominaga M, Yokota E, Sonobe S, Shimmen T.** 2000. Mechanism of inhibition of cytoplasmic streaming by a myosin inhibitor, 2,3-butanedione monoxime. *Protoplasma* **213,** 46–54.

**Towbin H, Staehelin T, Gordon J.** 1979. Electrophoretic transfer of proteins from polyacrylamide gels to nitrocellulose sheets: procedure and some applications. *Proceedings of the National Academy of Sciences, USA* **76,** 4350–4354.

**Van Gestel KV, Kohler RH, Verbelen J-P.** 2002. Plant mitochondria move on F-actin, but their positioning in the cortical cytoplasm depends on both F-actin and microtubules. *Journal of Experimental Botany* **53,** 659–667.

**Voeltz GK, Prinz WA, Shibata Y, Rist JM, Rapoport TA.** 2006. A class of membrane proteins shaping the tubular endoplasmic reticulum. *Cell* **124,** 573–586.

**Voeltz GK, Rolls MM, Rapoport TA.** 2002. Structural organization of the endoplasmic reticulum. *EMBO Reports* **3,** 944–950.

**Volkmann D, Mori T, Tirlapur UK, Konig K, Fujiwara T, Kendrick-Jones J, Baluska F.** 2003. Unconventional myosins of the plant-specific class VIII: endocytosis, cytokinesis, plasmodesmata/pit-fields, and cell-to-cell coupling. *Cell Biology International* **27,** 289–291.

**Vugrek O, Sawitzky H, Menzel D.** 2003. Class XIII myosins from the green alga *Acetabularia*: driving force in organelle transport and tip growth? *Journal of Muscle Research and Cell Motility* **24,** 87–97.

**Wada M, Kagawa T, Sato Y.** 2003. Chloroplast movement. *Annual Review of Plant Biology* **54,** 455–468.

**Wang Z, Pesacreta TC.** 2004. A subclass of myosin XI is associated with mitochondria, plastids, and the molecular chaperone subunit TCP-1 alpha in maize. *Cell Motility and the Cytoskeleton* **57,** 218–232.

**Yokota E, Imamichi N, Tominaga M, Shimmen T.** 2000. Actin cytoskeleton is responsible for the change of cytoplasmic organization in root hair cells induced by a protein phosphatase inhibitor, calyculin A. *Protoplasma* **213,** 184–193.

**Yokota E, McDonald AR, Liu B, Shimmen T, Palevitz BA.** 1995*a*. Localization of a 170 kDa myosin heavy chain in plant cells. *Protoplasma* **185,** 178–187.

**Yokota E, Mimura T, Shimmen T.** 1995*b*. Biochemical, immunochemical and immunohistochemical identification of myosin heavy chains in cultured cells of *Catharanthus roseus*. *Plant and Cell Physiology* **36,** 1541–1547.

**Yokota E, Shimmen T.** 1994. Isolation and characterization of plant myosin from pollen tubes of lily. *Protoplasma* **177,** 153–162.

**Yokota E, Sonobe S, Orii H, Yuasa T, Inada S, Shimmen T.** 2001. The type and the localization of 175 kDa myosin in tobacco cultured cells BY-2. *Journal of Plant Research* **114,** 115–116.

**Yokota E, Yukawa C, Muto S, Sonobe S, Shimmen T.** 1999. Biochemical and immunocytochemical characterization of two types of myosins in cultured tobacco bright yellow-2 cells. *Plant Physiology* **121,** 525–534.

**Zachariadis M, Quader H, Galatis B, Apostolakos P.** 2001. Endoplasmic reticulum preprophase band in dividing root-tip cells of Pinus brutia. *Planta* **213,** 824–827.